

## Study of shape of the yrast line and deformation changes in gadolinium isotopes

N A Mansour<sup>1\*</sup> and A M Diab<sup>2</sup>

<sup>1</sup>Physics Department, Faculty of Science, Zagazig University, Zagazig, Egypt

<sup>2</sup>Radiation Control Division, NCNSRC, AEA, Cairo, Egypt

E-mail : nassif-mansour@hotmail.com

Received 27 September 2001, accepted 4 December 2002

**Abstract** : The Gamma ray studies of  $^{147}\text{Gd}$  nucleus had been performed previously on the basis of gamma-gamma coincidence, angular distribution and excitation function measurements. In this nucleus ( $N = 83$ ), two values for the effective moment of inertia are suggested which reproduce the energies of the non-yrast states, that are populated in the decay of the isomer. A comparison of the energy level patterns for the even gadolinium isotopes have been done by studying the changes in deformation through the so-called Gauge plots.

**Keywords** : Nuclear structure, yrast line, deformation, gauge space.

**PACS No.** : 21.10.-k

Transitional nuclei with proton numbers  $Z = 64-68$  and neutron numbers  $N = 82-86$  have recently attracted considerable attention. In a pioneering study, Del Zoppo *et al* [1] demonstrated the existence of high spin isomers that decay by  $\gamma$ -cascades of high multiplicity in several of these nuclei. The transitional  $N = 88$  isotopes are found to be characterized by a small prolate deformation at low spin, but a switch to oblate aligned particle non-collective yrast states occurs around  $I = 30\hbar$ , which is followed by return to moderate collectivity at yet higher spins ( $I > 40\hbar$ ).

The studied nucleus  $^{147}\text{Gd}$  with one valence neutron outside the  $N = 82$  shell is essentially spherical in its ground state and its low spin structure is understood on the basis of the spherical shell model [2]. The nucleus was studied through measurement of the gamma radiation from the  $^{122}\text{Sn}$  ( $^{30}\text{Si}, xn$ ) reaction at  $E_{\text{lab}} = 160$  MeV [3–5] by the Heidelberg double anti-compton spectrometer.

### Shape of the yrast line :

The experimental yrast level energies *versus*  $I(I + 1)$  for  $^{147}\text{Gd}$  are given in Table 1 [and plotted in Figure 1]. The excitation energies are reproduced on an average by straight line which start at  $I = 0$  with an excitation energy  $E_0$  until  $I = 41/2\hbar$ . The fluctuations indicate that the yrast angular momentum does not originate from collective rotation where one would expect a smooth behavior of the yrast line. The  $I(I + 1)$  dependence is characteristic for the rotation of a rigid body or the average yrast line of the Fermi gas [6]. The good agreement for high spin values may be taken as evidence of the fact that Fermi gas model is a good approach for the few particle excitations in this nucleus.

In Figure 1, the extracted value for the effective moment of inertia  $\mathfrak{I}_{\text{eff}}$  is  $88 \text{ MeV}^{-1}$  for  $17/2 \leq I \leq 41/2$  whereas for  $I \geq 43/2$ , the value is  $136 \text{ MeV}^{-1}$ . The clustering of high- $j$  orbital around the Fermi levels tends to decrease, the slope of the yrast line for spins less than the maximum possible

\*Corresponding Author

with valence nucleons. For larger spins on the other hand, the necessity of promoting particles across the  $Z = 64$  or  $N = 82$  gap will result in a steeper yrast line. An example of the latter effect may be seen in the sharp increase in the slope of the yrast line just beyond spin  $43/2 \hbar$  (Figure 1). This change in the slope of the yrast line at high spins can be interpreted as a shape transition from spherical to oblate.

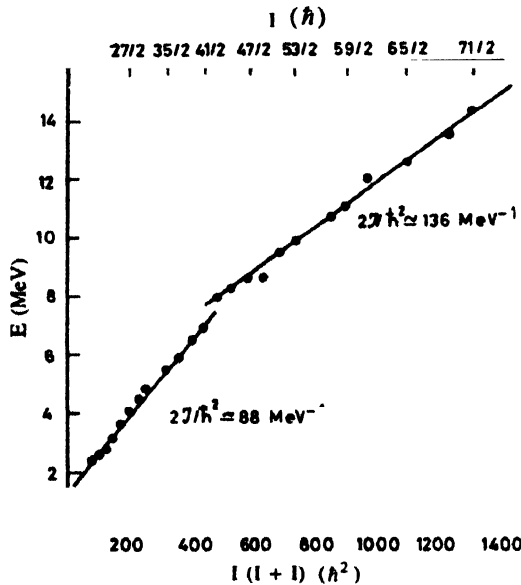


Figure 1. Excitation energies for yrast states in  $^{147}\text{Gd}$  with the corresponding  $I(I+1)$ .

Table 1. Excitation energies for yrast states in  $^{147}\text{Gd}$  [3–5] with the corresponding  $I(I+1)$ .

$E(\text{keV})$	$I$	$I(I+1)$	$E(\text{keV})$	$I$	$I(I+1)$
0.997	13/2	49	7.994	43/2	484
2.488	17/2	81	8.333	45/2	529
2.572	19/2	100	8.588	47/2	576
2.760	21/2	121	8.590	49/2	625
3.186	23/2	144	9.509	51/2	676
3.692	25/2	169	9.882	53/2	726
4.070	27/2	196	10.690	57/2	841
4.451	29/2	225	10.995	59/2	900
4.844	31/2	256	11.932	61/2	961
5.583	35/2	324	12.550	65/2	1089
5.923	37/2	361	13.448	69/2	1225
6.471	39/2	400	14.435	71/2	1296
6.906	41/2	441			

It seems that small oblate deformation ( $\beta = -0.1$  to  $-0.2$ ), shell effects and pairing correlations are responsible for the excess of the observed moments of inertia in  $^{147}\text{Gd}$  over the rigid sphere values.  $\mathfrak{J}_{\text{eff}}$  can be calculated from Mottelson and Valatin equation  $2\mathfrak{J}/\hbar^2 = 36/A^{5/3}$  [7], assuming the fact that the pairing vanishes and the moment of inertia reaches the rigid sphere values ( $\hbar^2/2\mathfrak{J} \approx 114 \text{ MeV}^{-1}$ ) at a deformation appropriate to  $\omega = 0$ .

#### Gauge plots and deformation changes :

The changes in deformations can be explored through the so-called 'Gauge plots' [8] of neutron number ( $N$ ) versus Fermi energy ( $\lambda$ ), in analogy to the plots of  $I_x$  versus  $\omega$ , which are frequently used for investigating rotational bands in ordinary space. In such a plot, one examines the difference in excitation energy  $E_x(I)$  for the ground-band members with spin ( $I$ ) in pair of neighboring even-even nuclei. This energy difference, together with the two nucleons separation energy  $S_{2n}$ , specifies the Fermi energy ( $\lambda$ ) as a function of spin. The Fermi energies are calculated from the relation

$$\lambda(N, I) = \frac{1}{2} [E_x(N+1, I) - E_x(N-1, I) - S_{2n}],$$

where  $N$  is the odd neutron number between the two even isotopes, which are compared. Figure 2 gives the results for the Gd nuclei calculated from the experimental energies [9–13] of the even isotopes with 82 to 90 neutrons [see also Table 2]. The separation energy ( $S_{2n}$ ) for each neutron number is taken from Ref. [14]. In this figure, we see a

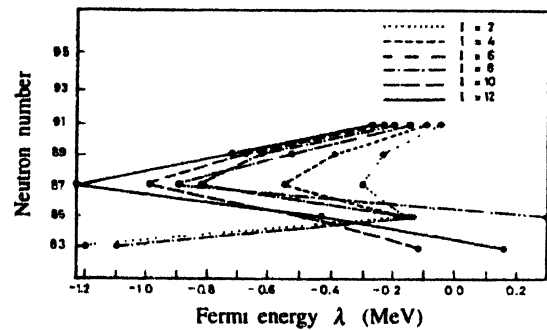


Figure 2. Back-bending plot showing the neutron number vs the Fermi energy for each spin in gauge space for the even Gd isotopes.

Table 2. Results of the Fermi energy ( $\lambda$ ) for isotopes  $^{147}\text{Gd}$  [9],  $^{149}\text{Gd}$  [10],  $^{151}\text{Gd}$  [11],  $^{153}\text{Gd}$  [12] and  $^{155}\text{Gd}$  [13].

	$\lambda$ (MeV)				
	$^{147}\text{Gd}$	$^{149}\text{Gd}$	$^{151}\text{Gd}$	$^{153}\text{Gd}$	$^{155}\text{Gd}$
2	-1.1964	-0.1621	-0.3092	-0.2361	-0.0491
4		-0.1441	-0.5482	-0.3991	-0.0981
6		0.2889	-0.9042	-0.5241	-0.1490
8	-1.6944	-0.1551	-0.8222	-0.6171	-0.1961
10	-0.1144	-0.4870	-1.0030	-0.6771	-0.2380
12	-0.1616	-0.4321	1.2360	-0.7141	-0.2770

pronounced irregularity around neutron number 88, which reminds very much about the backbending or upbending (depending on  $I$ ) behaviour.

The slope of the curves  $N(\lambda)$  reflects the level density at the Fermi surface. An upbend (for example) in this curve (i.e. an increase of slope in a small energy region), indicates a sudden increase in level density. This tends to be

energetically unfavorable and must therefore be compensated, most likely by a change in deformation, typically an increase. Thus, in such a case, the upper branch in the  $N(\lambda)$  curve is called the deformed branch (e.g.  $N > 89$  in Figure 2).

The calculation provides two values for the effective moment of inertia, which reproduces the energies of the non-yrast states that are populated in the decay of the isomer. In  $^{147}\text{Gd}$ , a change in the slope of the yrast line at high spins was found and interpreted as a shape transition from spherical to oblate form. Information on the energy level patterns through the so-called Gauge plots for the Gd isotopes with neutron numbers 82–90 clearly shows the backbend between the spherical and the deformed nuclei.

#### References

- [1] A Del Zoppo, C Agodi, R Alba, G Bellia, I Calabretta, R Coniglione, C Maiolino, E Migneco, P Piattelli, G Russo, P Sapienza and Yan Chen *Nucl. Phys.* **A476** 99 (1988)
- [2] J Borggan, G Sletten, S Bjornholm, J Pederson, A Del Zoppo, D C Radford, R V F Janssens, P Chowdhury, H Emling, D Frekers and T L Khoo *Nucl. Phys.* **A466** 361 (1987)
- [3] N Mansour, A Piepke, H Sanchez, A Moussavi, K Grotz, J Metzinger, H Strecker, H V Klapdor (MP If. Kern Physik HD) *50 Physikertagung der DPG and Frühjahrstagung* (Heidelberg, 17. Bis 21. März) p585 (1986)
- [4] N Mansour, A Moussavi, A Piepke, H Sanchez, J Metzinger and H V Klapdor (Max-Planck Institute für Kernphysik, Heidelberg, Germany) *International Symposium on Weak and Electromagnetic Interactions in Nuclei* (Heidelberg 1-5 July) p261 (1986)
- [5] A Moussavi *Dissertation* (Germany : Heidelberg) (1988)
- [6] A Bohr and B R Mottelson *Nucl. Str.* (New York : Benjamin) Vol. 2 (1975)
- [7] B R Mottelson and J G Valatin *Phys. Rev. Lett.* **5** 511 (1960)
- [8] M A Deleplanque, R M Diamond, F S Stephens, A O Macchiavelli and J E Draper and E L Dines *Nucl. Struct.* **A448** 495 (1986)
- [9] ( $^{147}\text{Gd}$ ) E Dafni, J Bendahan, C Broude, G Goldring, M Hass, E Naim, M H Rafailovich, C Chasman, O C Kistner and S Vajda *Nucl. Phys.* **A443** 135 (1985)
- [10] ( $^{140}\text{Gd}$ ) S Flibotte, B Hass, F Banville, J Gascon, P Taras, H R Andrews, D C Radford, D Ward and J C Waddington *Nucl. Phys.* **A530** 187 (1991)
- [11] ( $^{151}\text{Gd}$ ) E Hammaré, P Puhakka, A Siirola and T Tuurnala *Z. Phys.* **A272** 341 (1975)
- [12] ( $^{153}\text{Gd}$ ) P O Tjøm and B Elbeck *Mat. Phys. Medd. (Denmark)* **36** 3 (1967)
- [13] ( $^{154}\text{Gd}$ ) T Hayakawa, M Oshima, Y Hatsukawa, J Katakura, H Limura, M Matsuda, S Mitarai, Y R Shimizu, S-I Ohtsubo, T Shizuma, M Sugawara and H Kusakari *Nucl. Phys.* **A657** 3 (1999)
- [14] V A Kravtsov *Atomic Mass and Binding Energies for Nuclei* (Moscow : in Russian МОСКВА АТОМЭНАТ) (1974)